LETTERS

Coherent quantum state storage and transfer between two phase qubits via a resonant cavity

Mika A. Sillanpää[1], Jae I. Park[1] & Raymond W. Simmonds[1]

As with classical information processing, a quantum information processor requires bits (qubits) that can be independently addressed and read out, long-term memory elements to store arbitrary quantum states[1,2], and the ability to transfer quantum information through a coherent communication bus accessible to a large number of qubits[3,4]. Superconducting qubits made with scalable microfabrication techniques are a promising candidate for the realization of a large-scale quantum information processor[5–9]. Although these systems have successfully passed tests of coherent coupling for up to four qubits[10–13], communication of individual quantum states between superconducting qubits via a quantum bus has not yet been realized. Here, we perform an experiment demonstrating the ability to coherently transfer quantum states between two superconducting Josephson phase qubits through a quantum bus. This quantum bus is a resonant cavity formed by an open-ended superconducting transmission line of length 7 mm. After preparing an initial quantum state with the first qubit, this quantum information is transferred and stored as a nonclassical photon state of the resonant cavity, then retrieved later by the second qubit connected to the opposite end of the cavity. Beyond simple state transfer, these results suggest that a high-quality-factor superconducting cavity could also function as a useful short-term memory element. The basic architecture presented here can be expanded, offering the possibility for the coherent interaction of a large number of superconducting qubits.

A particularly interesting quantum information architecture involves the interaction of atoms with optical or microwave cavities having discrete electromagnetic modes, or cavity quantum electrodynamics (QED). Cavity QED systems[14,15] have enabled fundamental tests of quantum mechanics, as well as demonstrations of quantum memory and a quantum bus[16]. Recently, the Cooper pair box[5] has been successfully incorporated into a superconducting resonant cavity in order to perform analogous experiments in the strong coupling regime, generating a new field of study known as circuit QED[17–21]. Similar resonant cavities have been used to stabilize flux qubits[22]. Thus far, experiments have found spectroscopic evidence for the entanglement between two phase qubits and a resonator[23]. In this circuit QED experiment, we report the first time-domain measurements showing coherent interactions between two phase qubits and a cavity formed by a transmission-line resonator. Moreover, by coupling two phase qubits to a single cavity, taking advantage of the independent control of each phase qubit and single-shot readout, we have constructed an elementary quantum memory and quantum bus in a superconducting system.

For a flux-biased Josephson phase qubit[24], the ground state $|g\rangle$ and the first excited state $|e\rangle$ are encoded in the phase difference δ across a large-capacitance superconducting Josephson junction placed in a superconducting loop (Fig. 1a). These states resemble those of a simple harmonic oscillator but for the nonlinear, anharmonic potential[25] formed by the combination of the Josephson coupling energy $-E_J\cos(\delta)$ and the inductive energy stored in the superconducting loop, where E_J is the Josephson energy. Owing to their large capacitance, addressability, single-shot readout, and the ease with which the energy level separation $\hbar\omega = E_e - E_g$ can be tuned, phase qubits have proved to be relatively easy to couple together[11,23]. Superconducting qubits offer the possibility of forming a quantum processor with the help of communication channels or a 'qubus'.

Our superconducting quantum system is presented in Fig. 1b, c. Both qubits A and B are inductively coupled to two separate flux bias coils: one set of coils is used to adjust a static, direct-current (d.c.) flux bias, whereas the other set of radio-frequency coils, with a bandwidth from d.c. up to about 20 GHz, enables rapid flux bias changes ('shift pulses'), inductively coupled microwave pulses, and a fast measurement pulse. Each set of qubit d.c. flux bias lines includes low-pass and copper powder filters, while each set of radio-frequency flux pulsed lines are combined into a single microwave coaxial line at room temperature and attenuated by roughly 40 dB inside the cryostat. Microwave pulse control is performed with passively filtered (roughly gaussian-shaped pulses) and standard microwave mixers. Independently addressable state readout is accomplished via inductively coupled d.c. superconducting quantum interference devices (SQUIDs).

Our resonant cavity is an open-ended coplanar waveguide whose lowest-standing-wave eigenmode ($\lambda/2$-mode) has voltage maxima at each end of the waveguide (Fig. 1b). At near-resonance, this waveguide acts like a parallel, lumped element resonant LC circuit or cavity (Fig. 1c). The $\lambda/2$-mode forms a simple harmonic oscillator with an energy $\hat{H}_r = \hbar\omega_r\left(\hat{a}^\dagger\hat{a} + \frac{1}{2}\right)$ at the frequency $\omega_r/2\pi = 1/2\pi\sqrt{LC} \approx 8.74$ GHz, where $L = 2Z_0/\pi\omega_r$ and $C = \pi/2\omega_r Z_0$ represent their lumped element equivalents, $Z_0 \approx 50\,\Omega$ is the characteristic impedance of the coplanar waveguide, and the raising and lowering operators $\hat{a}^\dagger$ and $\hat{a}$ increase or decrease the photon number in the cavity.

Using the rotating-wave approximation, the hamiltonian of our quantum system formed by a single resonant cavity coupled at both ends to qubits A and B has the form of the Jaynes–Cummings hamiltonian[14,15] familiar from quantum optics

$$\hat{H} = \hat{H}_r + \sum_{j=\mathrm{A,B}} \hat{H}_j + \sum_{j=\mathrm{A,B}} \hbar g_j\left(\hat{a}^\dagger\hat{\sigma}^j_- + \hat{a}\hat{\sigma}^j_+\right) \qquad (1)$$

where $\hat{H}_j = \frac{1}{2}\hbar\omega_j\hat{\sigma}^j_+\hat{\sigma}^j_-$ is the single-qubit hamiltonian, $\hat{\sigma}^j_+\left(\hat{\sigma}^j_-\right)$ is the raising (or lowering) operator for creating (or annihilating) excitations in the jth qubit, and $\hbar\omega_j$ is controlled by the amplitude of the d.c. and radio-frequency flux bias. The interaction energy $2g_{\mathrm{A,B}} \approx \omega_r\left(C_c\Big/\sqrt{CC_J^{\mathrm{A,B}}}\right)$ was designed to be large enough to ensure that the timescale of quantum state transfer, $\pi/g_{\mathrm{A,B}} \approx 10$ ns, would

[1]National Institute of Standards and Technology, 325 Broadway, Boulder, Colorado 80305, USA.

not be limited by the relaxation times of either qubit or the cavity, putting this experiment in the strong coupling regime ($g_{A,B} > \gamma_{A,B} > \kappa$) for circuit QED[19] with qubit decay rates of $\gamma_A \approx 20$ MHz and $\gamma_B \approx 5$ MHz, and a cavity decay rate of $\kappa/2\pi \approx 1$ MHz.

When a single qubit is on-resonance with the cavity, so that the detuning is $\Delta = \omega - \omega_r = 0$, the individual eigenstates of the cavity ($|0\rangle$,$|1\rangle$) and the qubit ($|g\rangle$,$|e\rangle$) are no longer the eigenstates of the coupled system. Here, we find new eigenstates formed by an equal combination of cavity photons and qubit excitations, leading to the symmetric and antisymmetric superpositions $(|0\rangle|e\rangle \pm |1\rangle|g\rangle)/\sqrt{2}$. We also find that the energy-level separation of the new eigenstates, $\hbar(\omega \pm g)$, shows the typical vacuum-Rabi mode splitting. In addition, the exchange of photons between the cavity and a single qubit is strongest on-resonance.

In a familiar cavity QED experiment, an atom is excited, $|e\rangle$, and then interacts with an empty cavity, $|0\rangle$. The initial coupled-system state $|0\rangle|e\rangle$ begins to oscillate in time according to $\cos(gt)|0\rangle|e\rangle - i\sin(gt)|1\rangle|g\rangle$, so that the atom excitation $|e\rangle$ is transformed into a cavity photon $|1\rangle$ after a time $t = \pi/2g$ set by the interaction energy $\hbar g$. This continues coherently, with the photon continuously being transferred back and forth between the atom and the cavity in a process known as vacuum-Rabi oscillations. In typical atom–cavity systems[14,15], the interaction time is controlled by the atom's velocity through the cavity. In our analogous phase qubit–cavity system, we have the flexibility of using fast (~1 ns rise time), roughly rectangular flux bias shift pulses to adjust the interaction time (pulse width) and detuning Δ (pulse amplitude).

As a first demonstration of strongly coupled circuit QED in our system, these two basic vacuum-Rabi behaviours were independently verified for qubit A and qubit B. In Fig. 2a, we show an example of the vacuum-Rabi splitting for qubit B (a similar splitting was obtained for qubit A) using well-established spectroscopic techniques[24,26]. Vacuum-Rabi oscillations were also obtained for both qubits using an analogous technique borrowed from quantum optics[27] and used previously for a superconducting flux qubit coupled to a lumped-element cavity[21]. With qubit B fixed at a given detuning Δ_B, a fast (~4 ns) π pulse was applied to qubit B, preparing the initial coupled-system state $|0\rangle|e\rangle_B$. After a short interaction time, the state of the qubit is measured using a fast bias pulse in a manner identical to previous coupled-phase qubit experiments[11,26].

In Fig. 2b, we show an example of vacuum-Rabi oscillations for qubit B (similar oscillations were obtained for qubit A) for various detunings Δ_B with a raw contrast of ~20%, visible out to 200 ns. We see an increase in the vacuum-Rabi frequency with detuning, roughly proportional to $\sqrt{4g_B^2 + \Delta_B^2}$, with a minimum value on-resonance ($\Delta_B = 0$). An additional energy splitting, near the cavity resonance (seen in Fig. 2a on the lower spectroscopic branch) caused by a two-level system (TLS) defect common to large-area Josephson phase qubits[24,26], is responsible for a slight broadening of the spectroscopic splitting and a beating in the oscillations centred at $\Delta_B/g_B \approx 0.5$. Numerical calculations taking into account the size and position of the TLS agree well with the data for $g_B/\pi \approx 86$ MHz, where a small amount of beating is still visible on-resonance (see the inset of

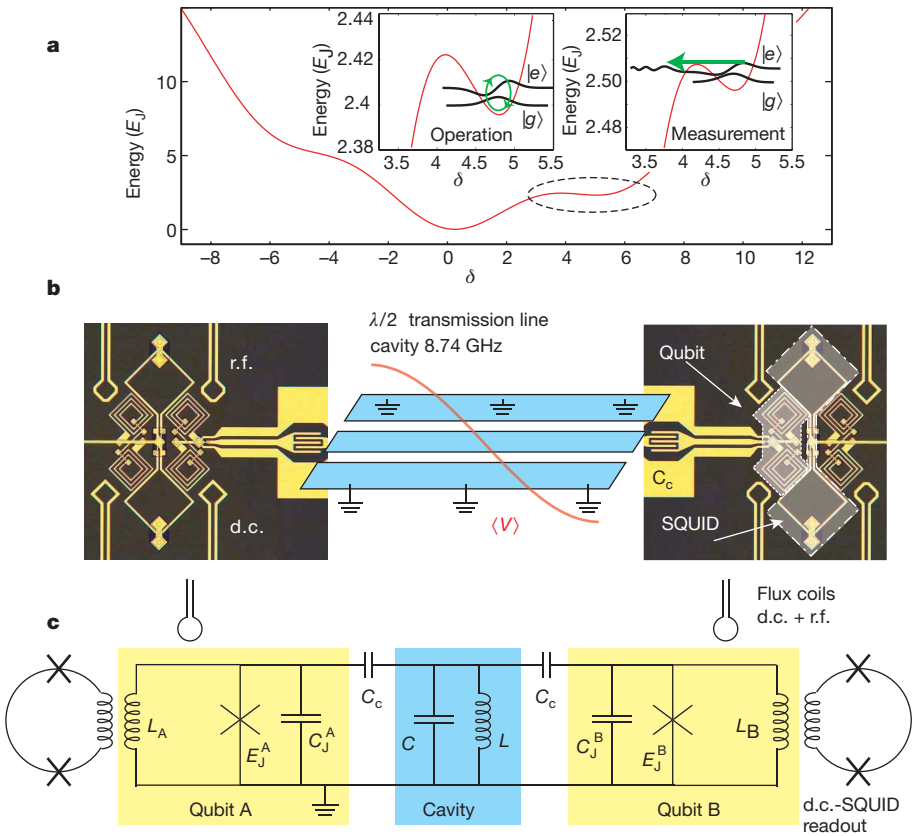

Figure 1 | Schematic description of the experiment set-up. a, Potential-energy diagram of the phase qubit (red line) and illustration of the operation and measurement (green line), where tunnelling of the qubit excited state $|e\rangle$ results in a difference of about one flux quantum in the loop, which is read out by a d.c. SQUID[24]. Repeated simultaneous single-shot measurements[11] (typically 1,000 events per data point) provides the necessary statistics to determine the excited-state population P_A and P_B of qubits A and B. **b**, Illustration of the quantum memory element with two Josephson phase qubits (with junction areas ~14 μm^2) connected via coupling capacitors $C_c \approx 6.2$ fF to either end of a resonant cavity formed by a 7-mm-long slowly meandering coplanar waveguide, with the qubits separated by about 1.1 mm. The red line depicts the voltage amplitude of the lowest $\lambda/2$-mode. The device was fabricated with standard optical lithography, producing Al/AlO_x/Al junctions on a sapphire substrate, using SiN_x as an insulator between the metallic layers. r.f., radio frequency. **c**, Lumped element equivalent circuit near the $\lambda/2$ resonance. The cavity has an effective inductance $L \approx 580$ pH and capacitance $C \approx 0.57$ pF, and both qubits had roughly $L_{A,B} \approx 690$ nH, $E_J^{A,B} \approx 45$ K and $C_J^{A,B} \approx 0.7$ pF.

Fig. 2b). Both qubits showed similar behaviour (without a nearby TLS in qubit A), differing by less than 10%, with a coupling strength ($g_A \approx g_B$) matching the design values (see Fig. 1).

After calibrating the amplitude of the shift pulses separately, for both qubits at their far-detuned operation points, we re-measured the vacuum-Rabi oscillations using the shift pulse sequence described in Fig. 2c and confirmed that both experimental methods gave similar results. The raw contrast for the vacuum-Rabi oscillations and for microwave-driven Rabi oscillations on individual qubits (~40%, when far detuned from each other, from the cavity, and from TLS defects) are consistent with previous measurements of coupled interactions using similar phase qubits[11,26]. It is known that the presence of TLS defects reduces qubit quality and causes contrast loss[24,26,28]. During flux changes, the qubit frequency sweeps past TLS defects, inducing Landau–Zener transitions to the qubit ground state, reducing measurement contrast.

To investigate the transfer of quantum states through the resonant cavity, we use the vacuum-Rabi interaction of both qubits. The complete sequence (1) to (5) is described in Fig. 2c. Using the static d.c. flux bias coils, the phase qubits are completely detuned ($\Delta_{A,B} \approx 15g_{A,B}$) from the cavity and from each other to suppress any stray cavity and qubit interactions. (1) In this configuration, we prepare a superposition state for qubit A using a rapid microwave pulse. (2) Next, we apply a shift pulse to qubit A, placing it on-resonance with the cavity for a time duration t_A. With shift pulse speeds much greater than $g_A/2\pi$ but still much less than $\omega_A/2\pi$, we effectively preserve the initially prepared quantum state until $\Delta_A = 0$, when the vacuum-Rabi oscillations begin to mix the qubit–cavity states. (3) With the detuning of qubit A restored, we wait for a short storage time $t_S = 10$ ns. (4) Then, we use a second shift pulse to place qubit B on-resonance with the cavity for a time t_B. (5) Finally, we return qubit B to its fully detuned position and both qubits are measured simultaneously using a fast (~4 ns) flux bias measurement pulse[11,26] that reveals the four joint probabilities $P_{AB} = P_{gg}$, P_{eg}, P_{ge} and P_{ee}. For simplicity, we choose to focus our attention on the individual excited-state occupation probabilities $P_A = P_{eg} + P_{ee}$ and $P_B = P_{ge} + P_{ee}$.

For the experimental data shown in Fig. 3, we used the state transfer protocol as outlined in Fig. 2c with an initial microwave π pulse applied to qubit A to create a simple pure state $|e\rangle_A$ for transfer. Figure 3a, b shows data over a range of interaction times t_A and t_B. The population maxima (red colour) for P_B in the target qubit B in Fig. 3b satisfy the following conditions: whenever t_A is an odd half-multiple of a vacuum-Rabi period, qubit A has a low population (blue colour) for P_A and we see a corresponding vacuum-Rabi oscillation of P_B occurring in qubit B. The experimental data are in good agreement with theoretical calculations of equation (1) under ideal conditions (Fig. 3c, d).

For clarity, we have extracted a set of three curves from the colour plots of Fig. 3a and b (arrows) and displayed them in Fig. 3e and f. If both shift pulses last for a half-vacuum-Rabi period $\pi/2g_{A,B}$, then the qubit excitation is completely transferred into a cavity photon and the subsequent excited-state population P_A is low, while in the target qubit B, we simultaneously observe clear vacuum-Rabi oscillations (black curve). The fact that the oscillations start from a minimum indicates the presence of a photon in the cavity at the moment of state transfer to qubit B, as expected. Thus, the excitation must leave qubit A, enter the cavity, where it is stored for a short time, and then finally be deposited in qubit B. Repeating this experiment for a full vacuum-Rabi period ($t_A = \pi/g_A \approx 11.6$ ns, green curves) shows no oscillations

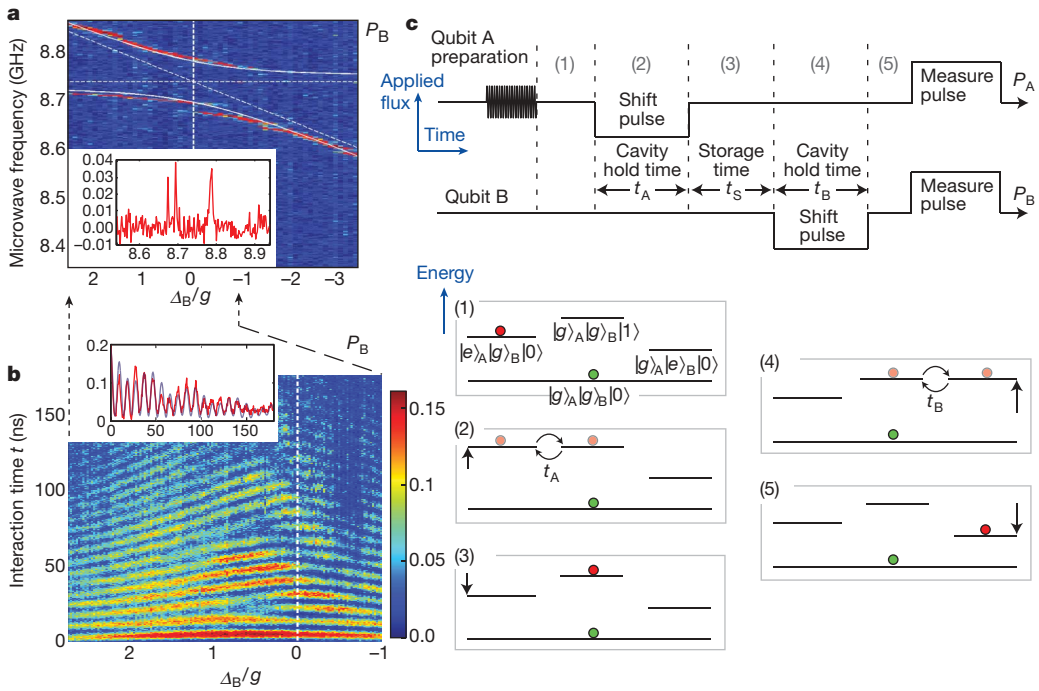

Figure 2 | Demonstration of strongly coupled circuit QED. a, Microwave spectroscopy of qubit B showing the vacuum-Rabi splitting (qubit A detuned). Blue colour represents low P_B, red represents high P_B. The inset shows a cross-section at $\Delta_B = 0$ (along the dashed vertical line). **b**, Vacuum-Rabi oscillations in qubit B after a short π pulse. The inset shows a cross-section at $\Delta_B = 0$. The blue line shows the numerical results including the TLS defect at near-resonance. **c**, Illustration of the general quantum state transfer protocol performed by a sequence of flux bias pulses applied to qubits A and B. Here each qubit is effectively decoupled from the cavity, except during the shift pulses, which bring them into resonance with the cavity, one qubit at a time. (1) An arbitrary superposition state $\alpha|g\rangle_A + \beta|e\rangle_A$ is prepared in qubit A. The red and green circles represent mixtures of the occupied energy levels. (2) Qubit A is shifted into resonance with the cavity for an interaction time lasting half of a vacuum-Rabi period, $t_A = \pi/2g_A$, the photon has been exchanged and the state of qubit A has been mapped into a superposition $\alpha|0\rangle + \beta|1\rangle$ of the two lowest-photon-number eigenstates (Fock states) of the cavity. (3) Qubit A is shifted off-resonance, storing the initial state in the cavity for a time duration t_S. (4) Qubit B is shifted into resonance for half of a vacuum-Rabi period, $t_B = \pi/2g_B$, transferring the state into qubit B, leaving the cavity in its ground state $|0\rangle$. (5) Both qubits are detuned, completing the coherent quantum state transfer from qubit A to qubit B.

in P_B, also as expected, because the photon was fully returned to qubit A (as indicated by higher values of P_A), leaving the cavity empty. The red lines illustrate an intermediate case, with $t_A \approx 3/4$ of a vacuum-Rabi period yielding oscillations of lower amplitude but the same frequency. Thus, we conclude that we can clearly transfer photons between two phase qubits, through the resonant cavity, as well as store this quantum information for a short time. By performing single-photon transfers for longer and longer storage times, we find a energy decay time of $\sim$1 μs for the cavity. Superconducting cavities are simple and tend to be more coherent than state-of-the-art superconducting qubits. With high-quality-factor superconducting microwave resonators[14,29], photon lifetimes near 100 μs could provide us with a feasible short-term memory element for use in superconducting quantum information systems.

To verify that quantum coherence is maintained during state transfer for an arbitrary superposition state, we perform a Ramsey fringe-type interference experiment[7] that preserves the quantum state up to a relative phase factor. We follow a protocol (Fig. 4a) similar to that used previously, except that here, we first prepare qubit A in an equal-weight superposition state $\left(|g\rangle_A + |e\rangle_A\right)/\sqrt{2}$, using a $\pi/2$ pulse applied slightly off-resonance, $\Delta\omega_A = \omega_d - \omega_A$, where ω_d is the microwave drive frequency. Again, we perform shift pulses, first, to map the initial state onto a superposition of the two lowest-photon-number states $|0\rangle$ and $|1\rangle$ of the cavity and, second, to retrieve this quantum information through the transfer to the states $|g\rangle_B$ and $|e\rangle_B$ spanned by qubit B. Owing to the short, but finite, time duration of the shift pulses and a brief storage time delay in the cavity, the state transferred to qubit B becomes $\left(|g\rangle_B + \exp(i\Theta)|e\rangle_B\right)/\sqrt{2}$ where Θ represents a trivial phase accumulation during the transfer process correctable by single-qubit rotations. Following the coherent state transfer to qubit B, we expect a clear precession of the transferred state during the time delay Δt. By applying a final $\pi/2$ pulse to qubit B (also slightly off-resonance, $\Delta\omega_B = \Delta\omega_A$), we complete the Ramsey fringe-type experiment, rotating qubit B into a different state depending on the total relative phase shift accumulated over the time Δt. In Fig. 4b and c, we show the expected Ramsey-type oscillations with frequencies linearly proportional to the microwave detuning $\Delta\omega_B$, thus verifying the transfer of quantum coherence through the cavity qubus.

To test the integrity of our experimental design, we investigated in detail the possible role of stray unintended photon generation in the cavity, both d.c. and radio-frequency inductive flux cross-coupling between the two qubits, the role of nearby TLS defects, and measurement cross-talk[11] directly through the cavity. First, we verified that the experiment satisfied basic consistency checks based on predictions of the model hamiltonian, equation (1), by altering the transfer pulse sequence shown in Fig. 2c. When we applied π pulses to either qubit with any of the shift pulses omitted, we saw no visible oscillations (above 1% contrast) in the target qubit. When compared to the $\sim$20% contrast of the full state transfer sequence, this corresponds to less than 0.05 stray photons in the cavity per π pulse, while the expected thermal occupation of the cavity with $\hbar\omega_r \approx 420$ mK at $T < 100$ mK should be $n < 0.02$. Next, we determined the cross-coupling of shift pulses by studying the flux modulation of one qubit for flux applied to the other qubit. We found at most a 6% cross-coupling between the two qubits, allowing us to avoid bias pulse cross-talk for large detunings. We performed numerical simulations that included the finite coherence times of each qubit, nearby TLS defects and no additional cross-talk. These results agree with the data, as shown in Fig. 2b. Finally, we performed detailed time-delay measurements[11] to investigate the role of measurement cross-talk when qubits A and B were not measured simultaneously. These results show that the cavity acts like an extremely narrow bandpass filter (centred at ω_r) that helps to block either qubit from the broadband transient microwave radiation generated by the measurement process[11]. Moreover, the use of shift pulses ensures both qubits are far detuned during the measurement process, minimizing excitation errors from radiation at frequency ω_r passing through the cavity.

We have successfully coupled two superconducting Josephson phase qubits through a resonant microwave cavity and have

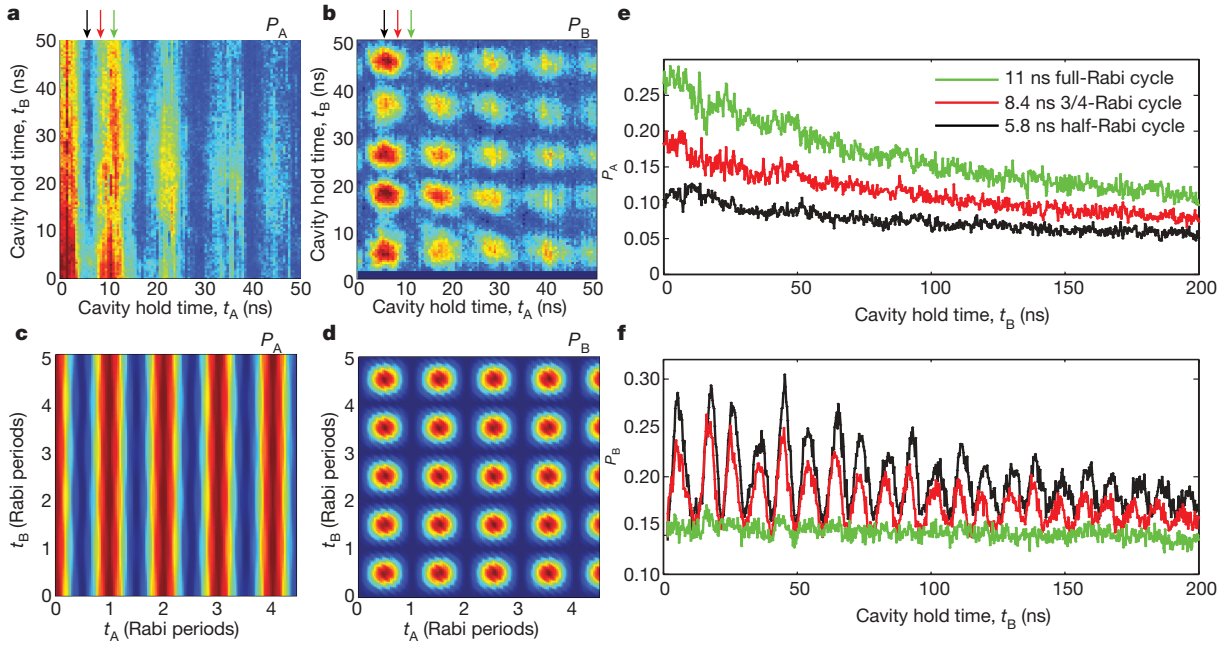

Figure 3 | Experimental data showing the quantum state transfer from qubit A to qubit B via the cavity. The transfer follows the protocol in Fig. 2, where the qubit A excited state $|e\rangle_A$ is first mapped into the single photon state $|1\rangle$ in the cavity, and then transferred into qubit B. **a**, **b**, Measured populations of qubits A and B as functions of the cavity hold times. Blue colour represents low $P_{A,B}$, red represents high $P_{A,B}$. **c**, **d**, Corresponding theoretical prediction for ideal conditions without decoherence and 100% fidelity. There is clear agreement between the experimental data and the ideal predictions, although qubit A was of lower quality than qubit B, most probably owing to fabrication imperfections. **e**, Excited-state occupancy P_A of the source qubit A reveals a lower population if the interaction time equals half of a vacuum-Rabi period, $t_A = \pi/2g_A \approx 5.8$ ns (black line). **f**, Simultaneous measurement of qubit B shows vacuum-Rabi oscillations induced by the transfer of a single photon (black line). Here the black, red and green curves in **e** (or **f**) correspond to data indicated by the arrows in **a** (or **b**); for a full discussion see the text.

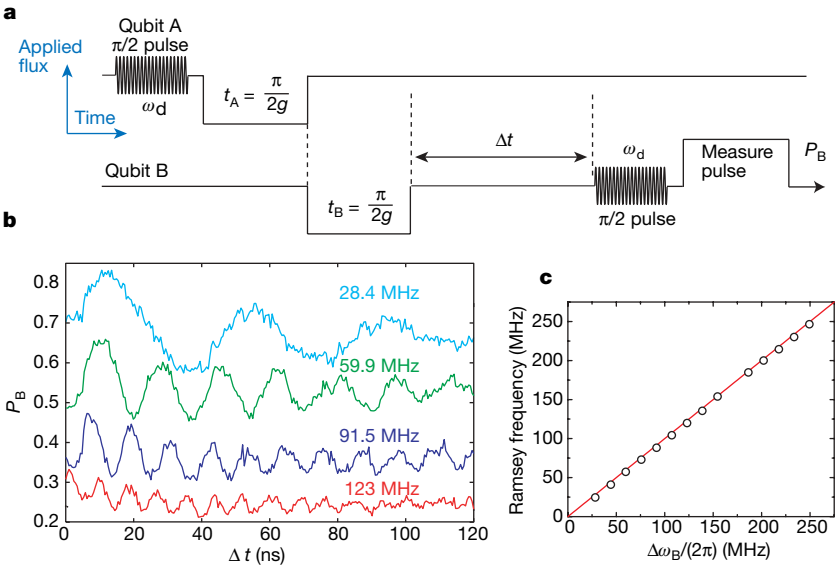

Figure 4 | Demonstration of the coherent transfer of a quantum state through the quantum bus. We use $\pi/2$ microwave pulses detuned from the level spacing frequencies $\omega_{A,B}$ of qubits A and B in order to perform a Ramsey fringe-type interference experiment. **a**, We prepare an equal-weight superposition state $(|g\rangle_A + |e\rangle_A)/\sqrt{2}$ in qubit A using a 10-ns-long $\pi/2$ pulse (with frequency ω_d) while both qubits are detuned from the cavity and from each other. We transfer this state into qubit B as in Fig. 2, and then wait for a delay time Δt before applying a detuned $\pi/2$ pulse to qubit B. This is analogous to Ramsey fringe experiments with single qubits, where a coherent quantum state slowly precesses at the microwave detuning frequency $\Delta\omega_B = \omega_B - \omega_d$. **b**, Coherent oscillations in qubit B for several detunings (vertically displaced for clarity). **c**, The frequency of the Ramsey-type oscillations as a function of the microwave detuning. The solid red line represents the theoretical predictions with no fitting parameters; circles are experimental data points.

observed vacuum-Rabi splittings, vacuum-Rabi oscillations, and the coherent transfer and storage of quantum states mediated by the cavity. The fidelity of the state transfer protocol is mostly limited by the quality of the phase qubits, the presence of TLS defects, and the non-optimization of the shape of the shift pulses performing the state transfer. We intend to improve qubit quality by eliminating dielectric materials and reducing the size of Josephson junctions to remove TLS defects[28,30]. Further measurements involving full state tomography[12,30] need to be performed to fully quantify the fidelity of this cavity qubus. This demonstration clearly shows progress towards the storage and communication of quantum information using coherent superconducting systems of multiple qubits, an exciting new frontier for solid-state circuit QED and quantum information science.

Received 18 April; accepted 25 July 2007.

1. Julsgaard, B., Sherson, J., Cirac, J. I., Fiurek, J. & Polzik, E. S. Experimental demonstration of quantum memory for light. *Nature* **432,** 482–486 (2004).
2. Langer, C. *et al.* Long-lived qubit memory using atomic ions. *Phys. Rev. Lett.* **95,** 060502 (2005).
3. Plastina, F. & Falci, G. Communicating Josephson qubits. *Phys. Rev. B* **67,** 224514 (2003).
4. Cleland, A. N. & Geller, M. R. Superconducting qubit storage and entanglement with nano-mechanical resonators. *Phys. Rev. Lett.* **93,** 070501 (2004).
5. Bouchiat, V. *et al.* Quantum coherence with a single Cooper pair. *Phys. Scr.* **T76,** 165–170 (1998).
6. Nakamura, Y., Pashkin, Yu. A. & Tsai, J. S. Coherent control of macroscopic quantum states in a single-Cooper-pair box. *Nature* **398,** 786–788 (1999).
7. Vion, D. *et al.* Manipulating the quantum state of an electrical circuit. *Science* **296,** 886–889 (2002).
8. Chiorescu, I., Nakamura, Y., Harmans, C. J. & Mooij, J. E. Coherent quantum dynamics of a superconducting flux qubit. *Science* **299,** 1869–1871 (2003).
9. Makhlin, Y., Schön, G. & Shnirman, A. Quantum-state engineering with Josephson-junction devices. *Rev. Mod. Phys.* **73,** 357–400 (2001).
10. Yamamoto, T., Pashkin, Y. A., Astafiev, O., Nakamura, Y. & Tsai, J. S. Quantum oscillations in two coupled charge qubits. *Nature* **425,** 941–944 (2003).
11. McDermott, R. *et al.* Simultaneous state measurement of coupled Josephson phase qubits. *Science* **307,** 1299–1302 (2005).
12. Steffen, M. *et al.* Measurement of the entanglement of two superconducting qubits via state tomography. *Science* **313,** 1423–1425 (2006).
13. Grajcar, M, *et al.* Four-qubit device with mixed couplings. *Phys. Rev. Lett.* **96,** 047006 (2006).
14. Schleich, W. P. & Walther, H. *Elements of Quantum Information* 1st edn, Ch. 1 (Wiley-VCH, New York, 2007).
15. Haroche, S. & Raimond, J.-M. *Exploring the Quantum: Atoms, Cavities, and Photons* 1st edn, Ch. 5 (Oxford Univ. Press, Oxford, 2006).
16. Maître, X. *et al.* Quantum memory with a single photon in a cavity. *Phys. Rev. Lett.* **79,** 769–772 (1997).
17. Buisson, O. & Hekking, F. W. J. in *Macroscopic Quantum Coherence and Quantum Computing* (eds Averin, D. V., Ruggiero, B. & Silvestrini, P.) 137–145 (Kluwer Academic, New York, 2001).
18. Blais, A., Huang, R.-S., Wallraff, A., Girvin, S. M. & Schoelkopf, R. J. Cavity quantum electrodynamics for superconducting electrical circuits: An architecture for quantum computation. *Phys. Rev. A* **69,** 062320 (2004).
19. Wallraff, A. *et al.* Strong coupling of a single photon to a superconducting qubit using circuit quantum electrodynamics. *Nature* **431,** 162–167 (2004).
20. Chiorescu, I. *et al.* Coherent dynamics of a flux qubit coupled to a harmonic oscillator. *Nature* **431,** 159–162 (2004).
21. Johansson, J. *et al.* Vacuum Rabi oscillations in a macroscopic superconducting qubit LC oscillator system. *Phys. Rev. Lett.* **96,** 127006 (2006).
22. Koch, R. H. *et al.* Experimental demonstration of an oscillator stabilized Josephson flux qubit. *Phys. Rev. Lett.* **96,** 127001 (2006).
23. Xu, H. *et al.* Spectroscopy of three-particle entanglement in a macroscopic superconducting circuit. *Phys. Rev. Lett.* **94,** 027003 (2005).
24. Simmonds, R. W. *et al.* Decoherence in Josephson phase qubits from junction resonators. *Phys. Rev. Lett.* **93,** 077003 (2004).
25. Martinis, J. M., Nam, S., Aumentado, J. & Urbina, C. Rabi oscillations in a large Josephson-junction qubit. *Phys. Rev. Lett.* **89,** 117901 (2002).
26. Cooper, K. B. *et al.* Observation of quantum oscillations between a Josephson phase qubit and a microscopic resonator using fast readout. *Phys. Rev. Lett.* **93,** 180401 (2004).
27. Brune, M. *et al.* Quantum Rabi oscillation: A direct test of field quantization in a cavity. *Phys. Rev. Lett.* **76,** 1800–1803 (1996).
28. Martinis, J. M. *et al.* Decoherence in Josephson qubits from dielectric loss. *Phys. Rev. Lett.* **95,** 210503 (2005).
29. Day, P. K., LeDuc, H. G., Mazin, B. A., Vayonakis, A. & Zmuidzinas, J. A broadband superconducting detector suitable for use in large arrays. *Nature* **425,** 817–821 (2003).
30. Steffen, M. *et al.* State tomography of capacitively shunted phase qubits with high fidelity. *Phys. Rev. Lett.* **97,** 050502 (2006).

Acknowledgements We gratefully acknowledge discussions with J. Aumentado, K. Cicak, K. Osborne, R. Schoelkopf and D. Wineland. This work was financially supported by the NIST and the DTO.

Author Information Reprints and permissions information is available at www.nature.com/reprints. The authors declare no competing financial interests. Correspondence and requests for materials should be addressed to R.W.S. (simmonds@boulder.nist.gov).